Scattering and Viscosimetric Behaviors of Four- and Six-Arm Star Polyelectrolyte Solutions

D. Moinard, R. Borsali,* D. Taton, and Y. Gnanou

Laboratoire de Chimie des Polymères Organiques, LCPO, CNRS, ENSCPB Université Bordeaux-1, 16 Avenue Pey Berland 33607 Pessac, France

Received March 9, 2005; Revised Manuscript Received June 6, 2005

ABSTRACT: This paper discusses the scattering and viscosity results of four- and six-arm sodium, cesium, and rubidium polyacrylate (PANa, PACs, PARb) star polyelectrolyte solutions in comparison with their equivalent linear polyelectrolyte chains. The polyelectrolyte effect is highlighted in these systems, and an estimate of the persistence length is deduced from static light scattering and X-ray scattering. Static and dynamic light scattering studies permitted to determine their mass average molar mass $\langle M_w \rangle$, their radius of gyration $\langle R_g \rangle$, their second virial coefficient A_2, their hydrodynamic radius R_H, and their persistence length L_P. The polyelectrolyte "abnormal" behavior was observed in the variation of the reduced viscosity η_{red} as a function of the polyelectrolyte concentration C_P on linear and star systems (existence of a maximum in η_{red} vs C_P). Additionally to the specific behavior brought by the star architecture, the results also show an important effect due to the type of counterions and the charge parameter on the scattering and the viscometric properties. A systematic comparison between linear and star polyelectrolytes having similar molar mass, counterions, and charge parameter is presented.

I. Introduction

Because of the presence of electric charges along the polymer chains, polyelectrolyte solutions exhibit different behaviors from those of neutral ones and lead to complex interactions, conformations, structures, and dynamics.[1−6] During the past decade, considerable experimental studies have been carried out to understand the properties of linear flexible and semiflexible polyelectrolyte systems using a wide range of techniques including scattering[7−11] and viscosity experiments.[12−17] Studies of the behavior of star-shaped polyelectrolytes remain, however, essentially theoretical,[18−21] except for a few data pertaining to small-angle X-ray scattering experiments[22,23] and very recent work by Ishizu and collaborators[24,25] on polyelectrolyte stars poly(*tert*-butyl acrylate)s (with high functionality $f = 30$ and $f = 97$) prepared by the atom transfer radical polymerization (ATRP) method. These authors have described the structural ordering of these stars using small-angle X-ray scattering (SAXS) in aqueous solution and found that such highly functional stars formed a bcc structure. The lack of experimental studies on star architectures is likely due to the fact that well-defined polyelectrolyte stars are not easily accessible. It is well-documented that star polymers can be obtained using ionic procedures following either the divergent or the convergent approaches.[26,27] Although successful, these methods are somehow limited to few categories of monomers. The breakthroughs witnessed in the past 10 years in controlled radical polymerization allow one to synthesize complex architectures including combs, dendrimer-like polymers, and stars without major difficulty.[28−30]

In this contribution, we discuss experimental results obtained on four- and six-arm polyelectrolyte stars based on acrylate units carrying different counterions (Na^+, Cs^+, Rb^+) using light scattering, X-rays, and viscosity experiments.

* Corresponding author: e-mail: borsali@enscpb.fr.

Owing to the high osmotic compressibility of polyelectrolyte solutions, the use of light scattering as a technique of characterization of star polyelectrolytes is not straightforward: the latter structure scatters less as compared to equivalent neutral polymer solutions. Additionally, no theory is available to describe the single chain conformation of polyelectrolyte stars in solution. One way to overcome this difficulty is to fully screen out the electrostatic interactions by addition of a simple electrolyte (such as NaCl) in order to use the scattering equations developed for neutral polymer systems. It is only under such conditions that information on individual macromolecule, such as mass-average molar mass $\langle M_w \rangle$, radius of gyration $\langle R_g \rangle$, second virial coefficient A_2, and form factor $P(q)$, can be determined. Besides the elastic properties, the hydrodynamical behavior in solutions (hydrodynamic radius R_H) can be determined using dynamic light scattering with or without added salt.

As for the persistence length of polyelectrolyte chains, experiments carried out at different added salt concentrations should lead to the determination of an estimate of the "apparent persistence" length as already described.[31] The term "apparent" is used because in such a method of data treatment, no excluded volume is taken into account. As suggested and studied by many authors,[32−35] in polyelectrolyte systems, the persistence length could be defined as a sum of two contributions which are (i) the intrinsic persistence length due to the intrinsic or "natural" rigidity of the backbone and (ii) the electrostatic persistence length arising from the repulsion between neighboring ionic sites that contributes to further stiffen the chain that strongly depends on the added salt concentration. The contribution due to the electrostatic persistence length approaches zero when enough salt is added, e.g., full screening of electrostatic interactions.

As to the variation of the reduced viscosity (η_{red}) as a function of the polyelectrolyte concentration C_P, it is known that "salt-free" dilute polyelectrolyte solutions

10.1021/ma050505f CCC: $30.25
Published on Web 07/06/2005

exhibit an "abnormal" behavior,[36] η_{red}, defined as $(\eta - \eta_0)/\eta_0 C_P$ (where η is the apparent viscosity of the solution, η_0 the viscosity of the solvent, and C_P the solution concentration) which presents a maximum in contrast to diluted neutral polymer solutions for which the reduced viscosity exhibits a linear variation with C_P. In the latter case, the intrinsic viscosity $[\eta]$ can be determined by the extrapolation of η_{red} to $C_P = 0$ using the following equations.

$$\frac{\eta_{SP}}{C_P} = [\eta] + K_H[\eta]^2 C_P + \ldots \qquad \text{Huggins equation} \tag{1}$$

$$\frac{\ln(\eta_r)}{C_P} = [\eta] - K_K[\eta]^2 C_P + \ldots \qquad \text{Kraemer equations} \tag{2}$$

Additionally, viscosimetric radii, R_V, can be estimated from $[\eta]$ as

$$R_V = \left[\frac{3}{10\pi N_A}\right]^{1/3} ([\eta] M_{app})^{1/3} \tag{3}$$

The existence of a maximum in the case of polyelectrolyte solutions makes such determination meaningless.[37]

The expansion effect[38] of the polyion chains in polyelectrolyte solutions is at the origin of the increase of η_{red} when the concentration decreases. Indeed, the screening effect due to the counterions becomes weaker when the polymer concentration decreases, and the polyion chains expand with the increase of intramolecular repulsive forces. This explanation qualitatively describes the increase of the η_{red} with decreasing C_P. Alternative explanations were also suggested,[37,39] but this peculiar behavior still remains an open issue. This abnormal viscosity behavior has been extensively studied over the past 40 years[16,39−41] for linear polyelectrolytes, but to our knowledge, no experimental data on star-shaped polyelectrolytes have been reported. To highlight the behavior of such architecture, we have measured the viscosity of PANa, PACs, and PARb stars and compared the η_{red} values with those measured for linear polyelectrolyte equivalents.

II. Experimental Section

II.1. Materials. Four-arm polysodium, polycesium, and polyrubidium acrylate (PANa, PACs, and PARb, respectively) stars were prepared using a combination of atom transfer radical polymerization (ATRP) and simple chemical modifications, as described in detail elsewhere.[23] We simply recall here that the four-arm poly(*tert*-butyl acrylate) PtBuA stars obtained from a tetrafunctional initiator were deprotected in poly(acrylic acid) stars before their neutralization by sodium, cesium, or rubidium hydroxide. Stars having six arms were synthesized following the same protocol using a hexafunctional initiator. Linear PtBuAs were purchased from PolymerExpert (France) with molar masses of 109 000 and 127 000 g/mol. They were modified to obtain linear polyelectrolytes following the protocol described above for PANa and PARb. Linear sodium poly(styrenesulfonate), NaPSS, was purchased from Fluka with a molar mass of 350 000 g/mol and studied for comparison. In Table 1 are listed the characteristics of all studied linear and star polyelectrolytes. A simple electrolyte (NaCl, CsCl, or RbCl) was added to the polyelectrolyte solutions in order to screen out the electrostatic interactions

II.2. Light Scattering Experiments. Dynamic light scattering (DLS) and static light scattering (SLS) experiments were performed using an ALV laser goniometer, which consists of a 22 mW HeNe linear polarized laser with 632.8 nm wavelength and an ALV-5000/EPP multiple tau digital correlator with 125 ns initial sampling time. The samples were kept at constant temperature (25.0 °C) during all the experiments. The accessible scattering angle range is from 10° up to 150°. However, most of the dynamic measurements were done at diffusion angles superior to 40°. The solutions were introduced into 10 mm diameter glass cells. The data acquisition was done with the ALV-Correlator Control Software.

Table 1. Characteristics of Polyelectrolyte NaPSS, PANa, PACs, and PARb Systems

architecture	sample[a]	counterion nature	DP[b]	$\langle M_n \rangle$, g/mol[c]	τ, %[d]
linear	NaPSS	sodium	1698	350 000	>90
	PANaL		840	75 302	81
	PARbL	rubidium	992	138 443	80
4-arm star	PANa4-1	sodium	617	56 614	91
	PANa4-2		860	77 613	83
	PACs4-1	cesium	617	117 608	90
	PACs4-2		860	145 797	74
	PARb4-3	rubidium	937	103 884	46
6-arm star	PANa6-1	sodium	624	57 856	95
	PACs6-1	cesium		122 917	95

[a] L refers to linear polymers while 4 and 6 denote the number of arm of the star polymers. [b] DP: degree of polymerization. [c] $\langle M_n \rangle$ calculated from molar mass of the corresponding PtBuA systems (except for PSSNa). [d] τ: sulfonation rate obtained by elementary analysis.

Solutions used for light scattering were prepared using the following method: the deionized water used as solvent was preliminarily filtered using a 0.1 μm Millipore syringe filter, and then the solutions were filtered directly into the cylindrical light scattering cells (2 mL volume) using a 0.22 μm Millipore syringe filter in order to eliminate the impurities and dust. The obtained results for our solutions at scattering angles <40° were not very accurate due to the use of water as the scattering medium. More reproducible and reliable data were obtained for higher angles and concentrations below the critical overlap concentration C_P^*. The scattered intensity $I(q)$ was calculated at different angles and was reported vs the wavevectors q defined as $q = (4\pi/\lambda_0)n \sin(\theta/2)$, where λ_0 is the wavelength of the incident beam, θ is the scattering angle, and n is the refractive index of the medium ($n_{water} = 1.33$).

Static Light Scattering. Static light scattering measurements were performed in the angular range from 40° to 140° by steps of 10°. The instrument automatically repeats the measurement until less than a predefined error (5%) is obtained. The refractive index increment (dn/dc) was measured for each system and was equal to 0.153, 0.116, and 0.077 mL/g for sodium, rubidium, and cesium star systems, respectively. Scattered intensities were normalized with toluene, and the solvent intensity was subtracted from all reported intensities.

Dynamic Light Scattering. The DLS autocorrelation functions have been measured for all studied polyelectrolyte systems in dilute solutions in a concentration range 1 g/L < C_P < 10 g/L and for angles between 40° and 130°. To avoid the electrostatic interactions, the experiments were performed in 1 M NaCl in some case. The analysis of the normalized intensity autocorrelation functions $C(q,t)$, where q is the scattering vector and t the time, was carried out following the method of cumulants, fitted with exponential decay functions. In the polyelectrolyte solution case, a double-exponential function characterizes $C(q,t)$. $C(q,t) = a + b[A_1 e^{-\Gamma_1 t} + A_2 e^{-\Gamma_2 t}]$ with Γ_1 and Γ_2 the relaxation frequencies of $C(q,t)$ at q value. An apparent diffusion coefficient D_i is related to each Γ_i: $D_i = \Gamma_i/q^2$. The concentration and angular dependence of Γ can be expressed as a first approximation to

$$\Gamma/q^2 = D_z(1 + k_D c + \ldots)(1 + A R_g^{\,2} q^2 + \ldots) \tag{4}$$

where D_z is the z-average diffusion coefficient, A is a parameter that is characteristic of the molecular architecture, and k_D is the effective interaction parameter. From the diffusion coefficient, the z-average hydrodynamic radius R_H can be calcu-

lated from the Stokes−Einstein equation $R_H = kT/(6\pi\eta D_z)$, where η is the solvent viscosity and kT the Boltzman energy factor.

II.3. Small-Angle X-ray Scattering (SAXS). Measurements were performed using the Nanostar SAXS system from Bruker-AXS with an X-ray source operating at 45 kV and 30 mA. The distance between the sample and the detector was 65 cm. The studied solutions were disposed in quartz capillaries having a diameter of 2 mm and measured during 15 h. The scattering intensities were corrected taking into account the detector response, the dark current, and the sample transmission. The data were plotted as a function of the magnitude of the scattering wavevector q defined in this case by the distance sample/detector and the size of the detector.

II.4. Viscosity Measurements. Steady shear experiments on star solutions prepared in a range of concentrations 0.001 g/mol < C_P < 10 g/mol were performed on RheoStress 300 (From ThermoHaake) with a double gap cylinder sensor system equipped with a temperature control system. All measurements were done at 22 °C. Most of the steady shear measurements were carried out at shear rates $\dot{\gamma}$ < 1000 s^{-1}. The apparent viscosity η was determined in "salt-free" solution and then in the presence of added salt in the mentioned range of concentrations.

III. Results and Discussion

III.1. Static Light Scattering. *Determination of A_2, $\langle M_w \rangle$, and $\langle R_g \rangle$.* Static light scattering was used to determine single chain parameters such as the mass-average molar mass $\langle M_w \rangle$, the radius of gyration $\langle R_g \rangle$, and the second virial coefficient A_2 using the Zimm method.[42] We performed static light scattering measurements on dilute polyelectrolyte solutions ($C_P \leq 10$ mg/mL) with added salt ($C_{salt} = 500$ mM) in order to screen out the electrostatic interactions and, consequently, use the Zimm formula. Typical Zimm plots for sodium polyacrylate PANa systems are shown in Figure 1a,b. Using the extrapolation at $C_P = 0$, the molar mass $\langle M_w \rangle$, the radius of gyration $\langle R_g \rangle$, and A_2 were calculated from the following equations:

$$\frac{kC_P}{I(q)} = \frac{1}{\langle M \rangle_w P(q)} + 2A_2C \tag{5}$$

$$\lim P(q)_{q\to 0} \cong 1 - \frac{q^2 R_g^{\,2}}{3} \tag{6}$$

$$\frac{kC_P}{I(q)} = \frac{1}{\langle M \rangle_w}\left[1 + \frac{q^2 R_g^{\,2}}{3}\right] + 2A_2C + \ldots \tag{7}$$

The results of the elastic light scattering obtained on the different investigated systems are listed in Table 2.

It is difficult to draw a general trend about the evolution of the second virial coefficient A_2 as a function of the functionality f or the counterion nature. However, one can note that A_2 is always positive (except for PANa4-2). Finally, the value of $\langle R_g \rangle$ for star systems is smaller than that of the equivalent linear: $\langle R_g \rangle_{PANa4-2} < \langle R_g \rangle_{PANaL}$ and $\langle R_g \rangle_{PARb4-3} < \langle R_g \rangle_{PARbL}$. Moreover one observes that $\langle R_g \rangle$ is decreasing with the star functionality for the same counterion and molar mass: $\langle R_g \rangle_{PANa6-1} < \langle R_g \rangle_{PANa4-1}$ and $\langle R_g \rangle_{PACs6-1} < \langle R_g \rangle_{PACs4-1}$. This result is expected since for the same molar mass and counterion $R_g^{\,2}{}_{STAR}/R_g^{\,2}{}_{LIN} = (3f-2)/f^2$. Also as expected, one observes that the radius of gyration increases with the counterion size for the same molar mass and functionality: $\langle R_g \rangle_{PANa4-1} < \langle R_g \rangle_{PACs4-1}$, $\langle R_g \rangle_{PANa4-2} < \langle R_g \rangle_{PACs4-2}$, and $\langle R_g \rangle_{PANa6-1} < \langle R_g \rangle_{PACs6-1}$.

Effect of Added Salt and Determination of the Persistence Length. Figure 2a,b shows typical variation of $KC/I(q)$ vs q^2 for dilute solutions of PARbL and PARb4−3 ($C_P = 2.5$ mg/mL) at different concentrations of added salt C_{salt}. The intensity of the scattered light increases markedly with the ionic strength, as expected for polyelectrolyte solutions. With the addition of salt C_{salt}, the intercept and the slope of $KC/I(q)$ vs q^2 decrease, indicating a decrease of both the second virial coefficient A_2 (eq 8) and the radius gyration R_g (eq 8).

$$A_2 = \left(\frac{1}{2C}\right)\left[\frac{KC}{I(q\to 0)} - \frac{1}{M_w}\right] \tag{8}$$

$$R_g^{\,2} = 3M_w \frac{d}{dq^2}\left[\frac{KC}{I(q)}\right] \tag{9}$$

As shown in Figure 2a,b, the electrostatic interactions are completely screened out with about 500 mM of added salt concentration C_{salt}, which causes an important effect on the scattered intensity.

A simple method to calculate an estimate of the "apparent" persistence length from the angular intensity of scattered light, as a function of added salt, has been already discussed by Reed[31] and Villetti et al.[43]

With such assumptions, the mean-square radius of gyration in the absence of excluded-volume effects is related to the persistence length of the polymer by the wormlike chain model:

$$R_{g0}^{\,2} = \frac{LL_t}{3} - L_t^{\,2} + \frac{2L_t^{\,3}}{L} - 2\left(\frac{L_t^{\,4}}{L^2}\right)\left[1 - \exp\left(\frac{-L}{L_t}\right)\right] \tag{10}$$

where L is the polymer contour length, $L_t = L_0 + L_e$ is the total persistence length, L_0 is the intrinsic persistence length, and L_e is the electrostatic persistence length. L_t can be deduced from the slope of $KC/I(q)$ vs q^2 assuming at first approximation that $L_t = 3R_g^{\,2}/L$, leading to

$$L_t = \frac{6m}{b}\frac{d\left[\frac{KC}{I(q)}\right]}{dq^2} \tag{11}$$

where m is the mass of monomer $m = 71$ g/mol (without taking the counterion mass into account) and $b = 2.56$ Å is the distance between monomers. Thus, the apparent persistence lengths were calculated for both linear and polyelectrolyte stars at different salt concentrations. The L_t values obtained at an infinite ionic strength are illustrated in Figure 3 where the variation of the apparent persistent length (L_t) as a function of the inverse square root of the ionic strength is plotted. The y-intercept yields the apparent intrinsic persistence lengths at infinite ionic strength. For linear sodium polyacrylate, the obtained value of 1.87 nm is very close to those published by Kitano et al.[44] (2 nm at $C_{salt} = 1.5$ M) and Tricot (2.1 nm at $C_{salt} = 0.5$ M)[33] and is slightly higher than the data reported by Muroga et al.[34] (between 0.9 and 1.4 nm depending on the ionic strength).

Affording a rough estimate, this method which is mainly valid for linear polyelectrolyte was applied to star architectures. It can, indeed, permit a direct comparison between two polyelectrolyte stars having the

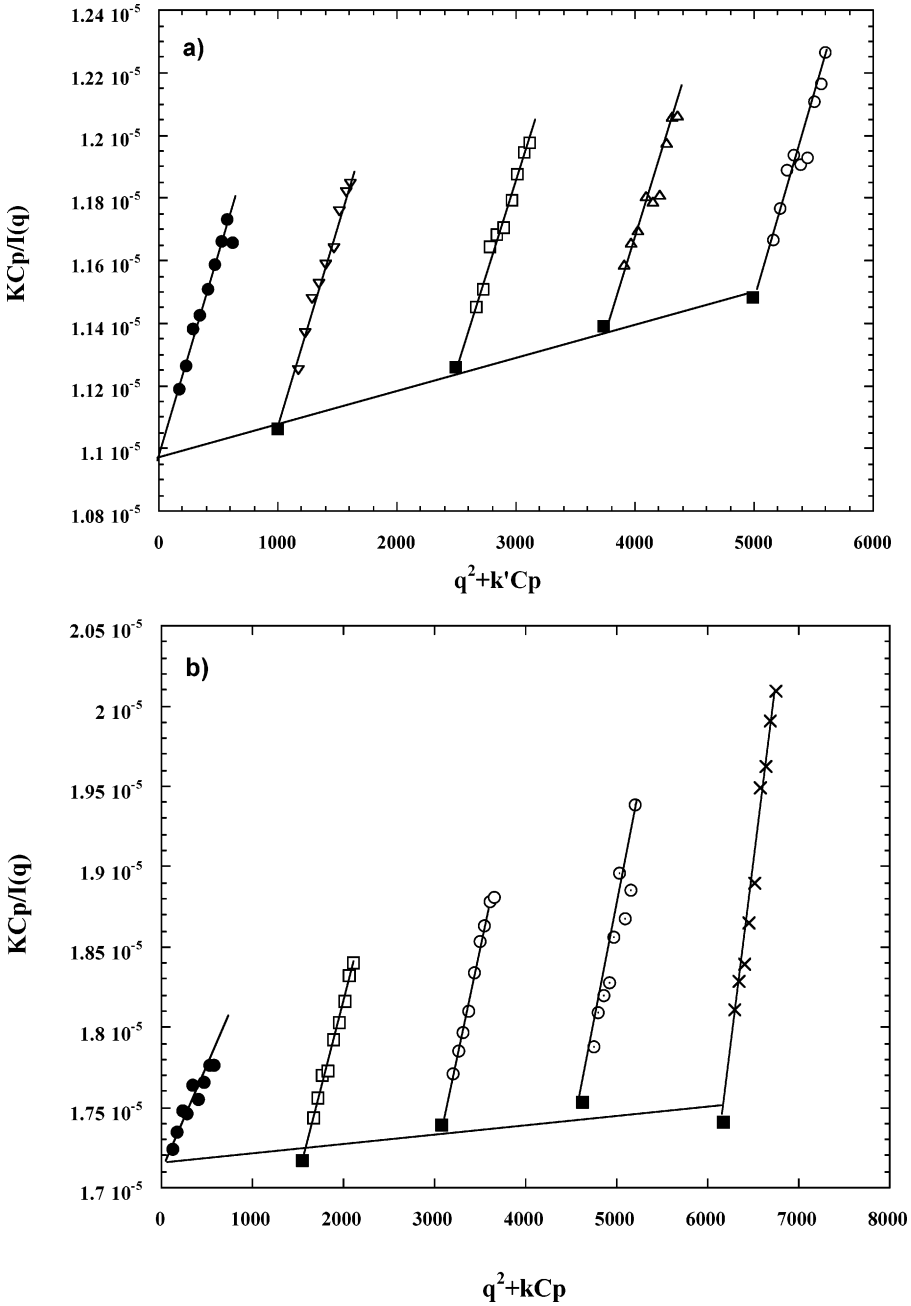

Figure 1. (a) Typical Zimm plot obtained for PANaL polyelectrolyte solutions with added salt (C_{salt} = 500 mM): ●, extrapolation at C_P = 0; ■, extrapolation at q = 0. ○, C_P = 5 mg/mL; △, C_P = 3.75 mg/mL; □, C_P = 2.5 mg/mL; ▽, C_P = 1 mg/mL. (b) Typical Zimm plot obtained for PANa6-1 polyelectrolyte solutions with added salt (C_{salt} = 500 mM): ●, extrapolation at C_P = 0; ■, extrapolation at q = 0. ×, C_P = 10 mg/mL; ⊙, C_P = 7.5 mg/mL; ○, C_P = 5 mg/mL; □, C_P = 2.5 mg/mL.

Table 2. Single Chain Parameters for Linear and Star PA Systems

system	DP	$\langle M_n \rangle$ without CI (g/mol)[a]	$\langle M_n \rangle$ with CI (g/mol)[b]	$\langle M_w \rangle$ (C_p = 0) (g/mol)[c]	$\langle M_w \rangle$ (q = 0) (g/mol)[d]	$\langle R_g \rangle$ (nm)	A_2 (mol cm^3 g^2)
linear							
PANaL	840	59 770	75 300	91 190	91 120	18.1	1.06×10^{-4}
PARbL	992	70 470	138 440	99 550	106 700	19	2.7×10^{-5}
4-arm star							
PANa4-1	617	43 780	56 610	51 000	50 090	14	1.1×10^{-4}
PACs4-1			117 600	58 190	58 130	14.7	8.1×10^{-5}
PANa4-2	860	61 000	77 610	70 060	70 060	16.1	-5.14×10^{-5}
PACs4-2			145 790	87 160	87 160	16.5	8.37×10^{-5}
PARb4-3	937	66 570	103 880	80 180	80 150	15.6	9×10^{-5}
6-arm star							
PANa6-1	624	44 200	57 850	58 270	58 270	13.7	5.6×10^{-5}
PACs6-1			122 920	75 120	75 130	14.2	8.3×10^{-5}

[a] $\langle M_n \rangle$ calculated from the molar mass of the corresponding PtBuA neutral systems without the counterion contribution (CI). [b] $\langle M_n \rangle$ calculated from the molar mass of the corresponding PtBuA neutral systems taking into account the counterion contribution (CI). [c] $\langle M_w \rangle$ obtained by extrapolation at C_P = 0. [d] $\langle M_w \rangle$ obtained by extrapolation at q = 0.

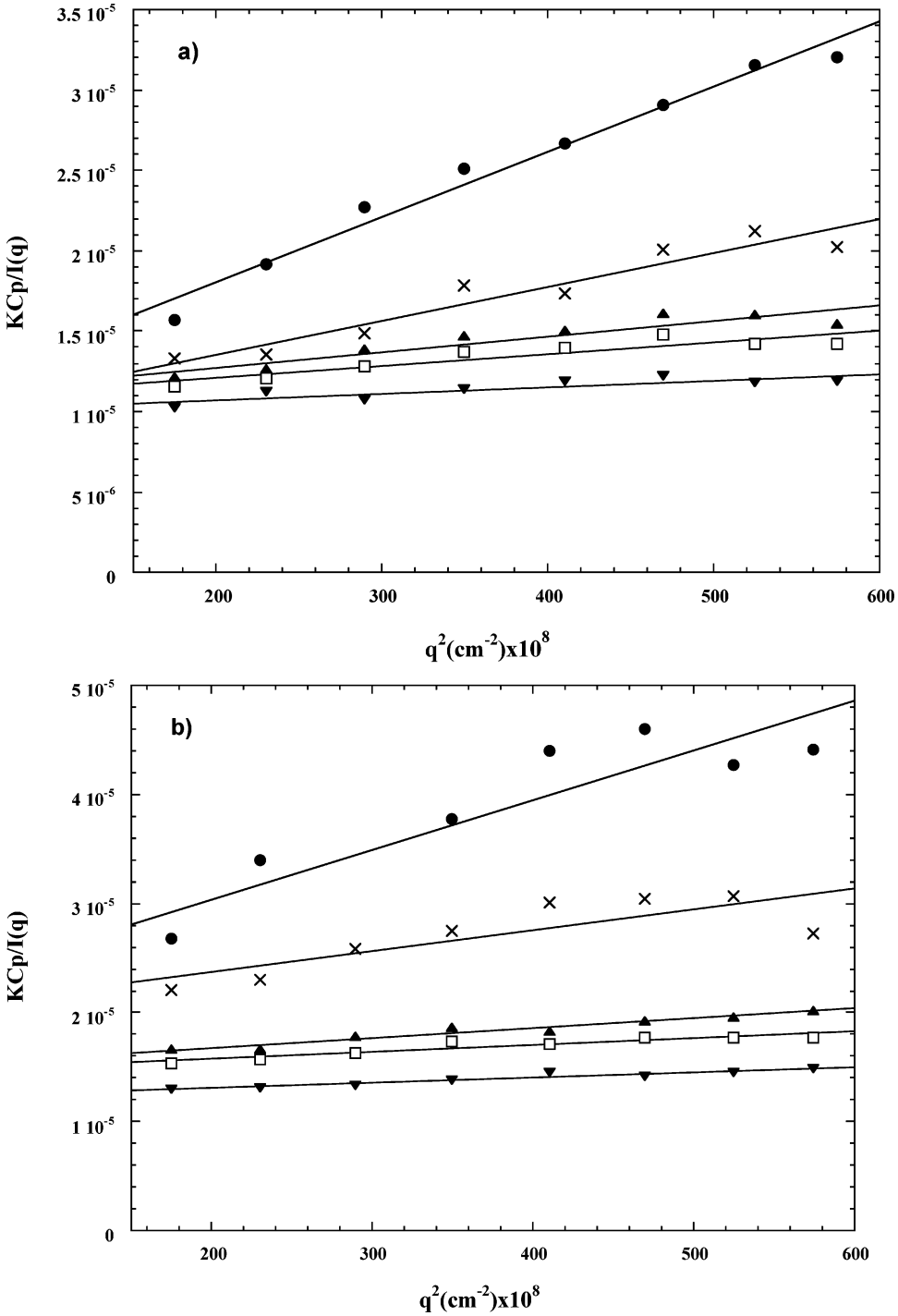

Figure 2. (a) Effect of added salt on PARbL polyelectrolyte solutions (C_P = 2.5 mg/mL). Data obtained using static light scattering at different salt concentration C_{salt}. ●, C_{salt} = 0 M; ×, C_{salt} = 0.01 M; ▲, C_{salt} = 0.05 M; □, C_{salt} = 0.1 M; ▼, C_{salt} = 0.5 M. (b) Effect of added salt on PARb4-3 polyelectrolyte solutions (C_P = 2.5 mg/mL). Data obtained using static light scattering at different salt concentration C_{salt}. ●, C_{salt} = 0 M; ×, C_{salt} = 0.01 M; ▲, C_{salt} = 0.05 M; □, C_{salt} = 0.1 M; ▼, C_{salt} = 0.5 M.

same arm length and different counterion such as PANa4-1 and PACs4-1. The obtained values are listed in Table 3.

One observes that polyelectrolyte stars exhibit a slightly higher L_p than that of linear homologues. This is due to the fact that each arm of the stars has a lower degree of freedom as compared to linear chains. Thus, one can infer that the star core imposes an extra "rigidity" leading to an increase of L_p. Moreover, our results show that the L_p value increases with the star functionality *f*. Indeed, systems having roughly the same DP and the same counterion give $L_{p,PANa4-1} < L_{p,PANa6-1}$ and $L_{p,PACs4-1} < L_{p,PACs6-1}$. When the functionality increases, the steric repulsions become more important near the star core and consequently the persistence length increases. As for the L_p values for PANa4−1 and PACs4−1 (same chain length), they are very close and independent of the nature of the counterion. Thus, the persistence length L_p increases as a function of the functionality and is approximately the same for different counterions (the effect of the counterion is not predominant since the determination of L_p has been carried out in excess of salt): $L_{p,linear} \sim 1.85$ nm, $L_{p,4-arm\ star} \sim 2.7$ nm, and $L_{p,6-arm\ star} \sim 3.1$ nm.

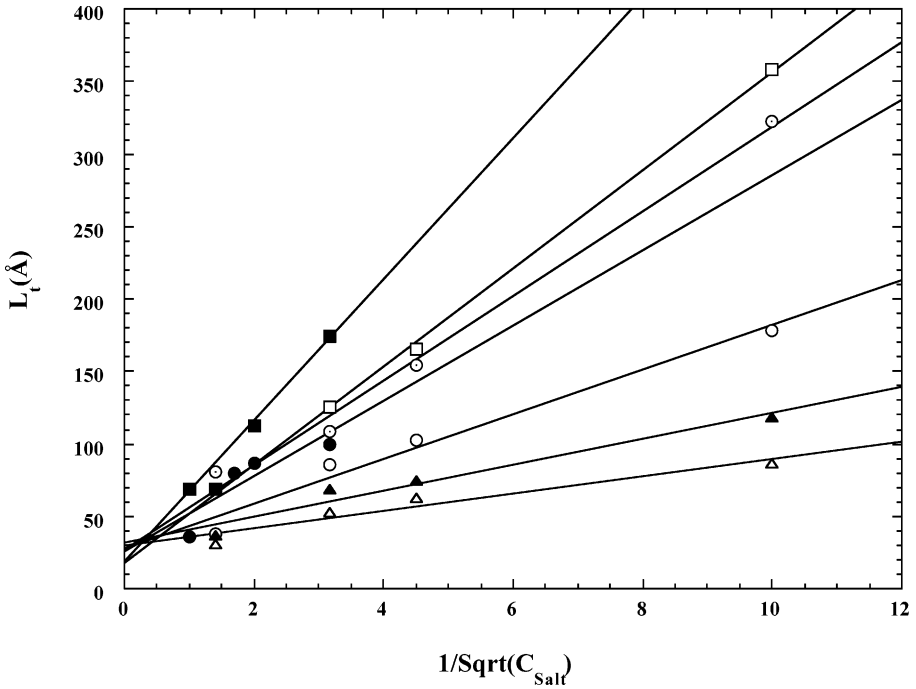

Figure 3. Persistence lengths as a function of added salt concentration C_{salt} obtained for different polyelectrolyte solutions: ■, PANaL; □, PARbL; ○, PACs4-1; ●, PANa4-1; ⊙, PARb4-3; ▲, PANa6-1; △, PACs6-1.

Table 3. Persistence Length Values Obtained Using Light Scattering for Different Polyelectrolyte Systems in Excess of Salt (C_{salt} = 500 mM)

	linear		4-arm stars			6-arm stars	
	PANaL	PARbL	PANa4-1	PACs4-1	PARb4-3	PANa6-1	PACs6-1
L_p (nm)	1.87	1.83	2.63	2.76	2.73	3.21	2.96

III.2. Dynamic Light Scattering. Dynamic light scattering experiments carried out on polyelectrolyte stars at different polyelectrolyte C_P and added salt C_{salt} concentrations show the existence of two relaxation modes both in dilute and semidilute regimes. As a representative example, the autocorrelation functions $C(q,t)$ and the particle size distribution obtained by CONTIN analysis of DLS data are shown in Figure 4 for the sample PANa4−2 at C_P = 1 g/L, in excess of added salt measured at the scattering angle 90°.

Two relaxation modes are generally observed in polyelectrolyte linear systems and have been reported by several authors[45,46] and studied in detail by Sedlak.[47] The first one is characterized by a fast relaxation, and the second one exhibits a slower relaxation time associated both a fast D_f and a slow D_s diffusion coefficient.

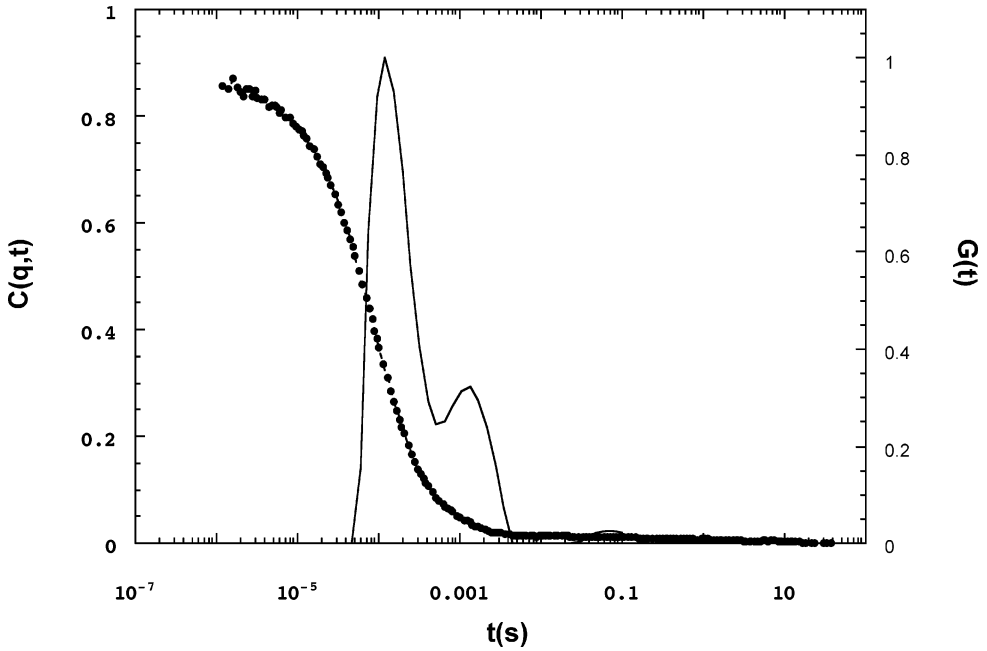

Figure 4. Autocorrelation functions and CONTIN analysis (full line) of PANa4-2 at C_P = 1 g/L in added salt excess (C_{salt} = 0.5 M) at 90°.

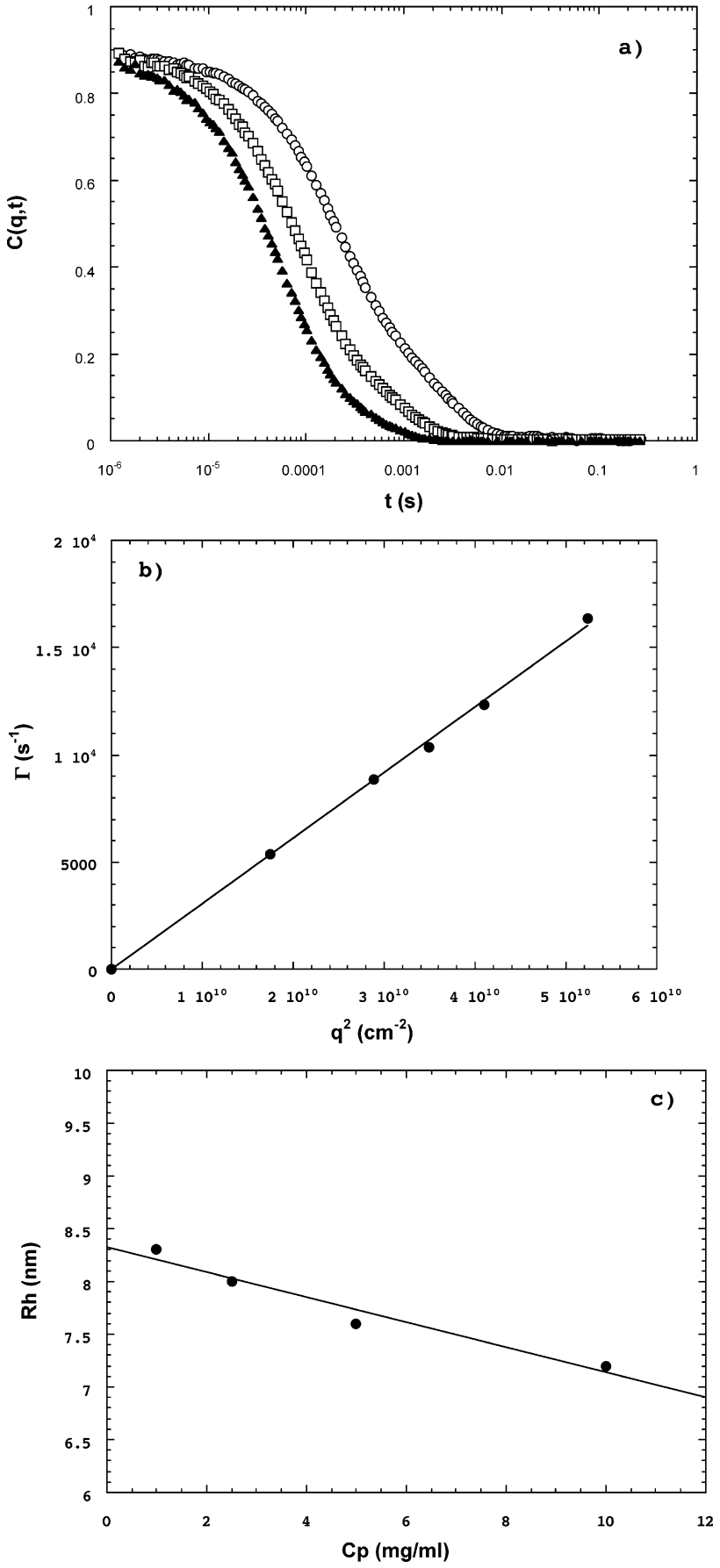

Figure 5. (a) Autocorrelation functions of PANa6-1 in the presence of 0.5 M NaCl added salt ($C_P = 2.5$ g/L) at different scattering angles. ○, $C(q,t)$ at 60°; □, $C(q,t)$ at 90°; ▲, $C(q,t)$ at 120°. (b) Dependence of the frequency (Γ) related to fast coefficient diffusion with the square magnitude of the scattering vector (q^2) in these conditions. (c) Concentration dependence of the hydrodynamic radius of PANa6-1 in the presence of 0.5 M NaCl added salt.

Table 4. Data of Dynamic Light Scattering Analysis

system		DP	R_g (nm)[a] $C_{salt} = 0.5$ M	R_H (nm)[b] $C_{salt} = 0.5$ M	R_g/R_H[c]	R_H (nm)[d] $C_{salt} = 0$ M	contraction (%)[e]
linear	PANaL	840	18.1	10.1	1.79	13.5	25
	PARbL	992	19	9.9	1.92	14	29
4-arm stars	PANa4-1	617	14	8.4	1.67	10.7	21
	PACs4-1		14.7	8.9	1.65	11.2	20
	PANa4-2	860	16.1	9.1	1.77	12.2	25
	PACs4-2		16.5	9	1.83	11.1	19
	PARb4-3	937	15.6	9.7	1.61	11.4	15
6-arm stars	PANa6-1	621	13.7	8.3	1.65	10.9	24
	PACs6-1		14.2	8.7	1.63	11.1	22

[a] R_g from static light scattering calculated from Zimm method (in added salt excess). [b] R_H calculated from correlation functions in dilute regime and in added salt excess $C_{salt} = 0.5$ M. [c] R_g/R_H ratio calculated from R_g and R_H in added salt excess $C_{salt} = 0.5$ M. [d] R_H calculated from correlation functions in dilute regime in "salt-free solutions" $C_{salt} = 0$ M. [e] Size variation (contraction) due to electrostatic interaction screening and calculated as $100 \times (1 - R_H(C_{salt} = 0.5\ M)/R_H(C_{salt} = 0\ M))$.

For linear polyelectrolyte systems, the first mode is related to the polyion chain dynamic, whereas the second mode is related to the aggregate dynamic though the origin of these aggregates is not completely understood and is still open for discussion. Consequently, it is not surprising that our star polyelectrolyte solutions do also present such a dynamical behavior. Our results show that these two modes are also sensitive to polyelectrolyte and added salt concentrations. The fast diffusion can be also attributed to polyion individual chains in dilute regime and permits to determine the hydrodynamic radii R_H.

In dilute solution ($C_P < C_P^*$), the fast coefficient diffusion allows to calculate R_H of studied polyelectrolyte systems from the Stokes−Einstein relation. For each system, the correlation functions were studied with and without added salt, and a typical example is illustrated in Figure 5. The results are listed in Table 4 for all the studied systems. Values of DP and R_g are also reported.

In excess of added salt, R_H increases with the degree of polymerization $R_{H,PANa4-1} < R_{H,PANa4-2}$ for systems having the same architecture and counterion. For systems having the same counterion, R_H decreases when the functionality decreases: $R_{H,PANa4-1} < R_{H,PANaL}$, $R_{H,PARb4-3} < R_{H,PARbL}$, $R_{H,PANa6-1} < R_{H,PANa4-1}$, and $R_{H,PACs6-1} < R_{H,PACs4-1}$. In these cases, the behavior of polyelectrolyte systems is comparable to that of a neutral polymer since the electrostatic interactions are screened out.

In "salt-free" solution, the same behaviors were observed regarding the R_H variation as a function of DP and functionality. It is important to recall that in such conditions measurements were difficult to carry out because of the presence of aggregates and the variation of R_H as a function of added salt for PANaL/PANa4-2 and for PACs4-1/PACs6-1 is illustrated in Figure 6. It is clearly observed that the variation of R_H as a function of C_{salt} is not influenced by the star architecture in these systems and rather due the screening of the electrostatic interactions listed in Table 4. For linear systems, the contraction due to the screening of electrostatic interaction is about 25% whereas the star systems exhibit a smaller average value due to the star core. The R_g/R_H ratio depends on the morphology of the studied system. Values close to 1.5−1.8 can be attributed to a statistical coil conformation. Our results show that R_g/R_H depends on the architecture: it decreases when the functionality increases for polyelectrolytes having comparable molar masses and the same counterion. Without taking the counterion into account, the average value is equal to 1.85 for linear polyelectrolytes, 1.7 for 4-arm stars, and 1.64 for 6-arm stars showing, and as expected, that the star polyelectrolyte systems are more "dense" as compared to their equivalent linear ones.

III.3. SAXS Experiments. *Experimental Determination of the Persistence Length*. Complementary experiments using SAXS were carried out on linear and star polyelectrolytes in order to determine the persistence length, in this case, from the variation of $I(q)$ vs q. Similarly to the light scattering study, SAXS experiments were carried out using an excess of added salt. At this stage, it is important to note that SAXS studies on "salt-free" systems present a maximum of $I(q)$ vs q (polyelectrolyte peak).[23] In excess of salt, therefore for a system behaving like a neutral polymer, it is possible to determine L_p using different methods including those described by Porod-Kratky,[48] des Cloiseaux,[49,50] Koyama,[51] or Burchard and Kajiwara.[52]

Indeed, SANS as well as SAXS is widely used for the determination of the form factor of polymer chains in different environments. The conformation of a semiflexible polyelectrolyte in excess of added salt (neutral behavior) is well described by the wormlike chain model of Kratky and Porod. In this model, it is assumed that the polymer chain has a Gaussian behavior at large scale and a rigid-rod conformation at short scale. The Kratky plot, i.e., $q^2I(q)$ vs q, for flexible polymer is characterized by three regions: Guinier, Debye, and rodlike behaviors.[34] The value of q at the cross over between the second and the third region (called q^*) is generally used to calculate the persistence length. In this representation and under such experimental conditions (excess of salt), $L_p = k/q^*$ can be determined, where k is a constant value equal to 1.91 according to Kratky[48] and Koyama[51] or equal to 2.87 according to Burchard and Kajiwara.[52] The effect of polymer concentration on the position of q^* has already been studied, and q^* is almost independent of polymer concentration even at C_P close to C_P^*, the overlap concentration.[34] In Figure 7, the Kratky representation is shown for sodium system solutions in excess of salt. From the same set of data, q^* can be also determined using the des Cloiseaux[49] method from the form factor $P(q)$ in the asymptotic range, i.e., at large scattering wave vector q value. For infinitely long chain the des Cloiseaux relation reads

$$P(q) = \frac{\pi}{qL} + \frac{2}{3q^2LL_p} \tag{12}$$

where L is the contour length of the polymer chain. At $qL_p > 1$ the form factor $P(q)$ exhibits the q^{-1} scattering

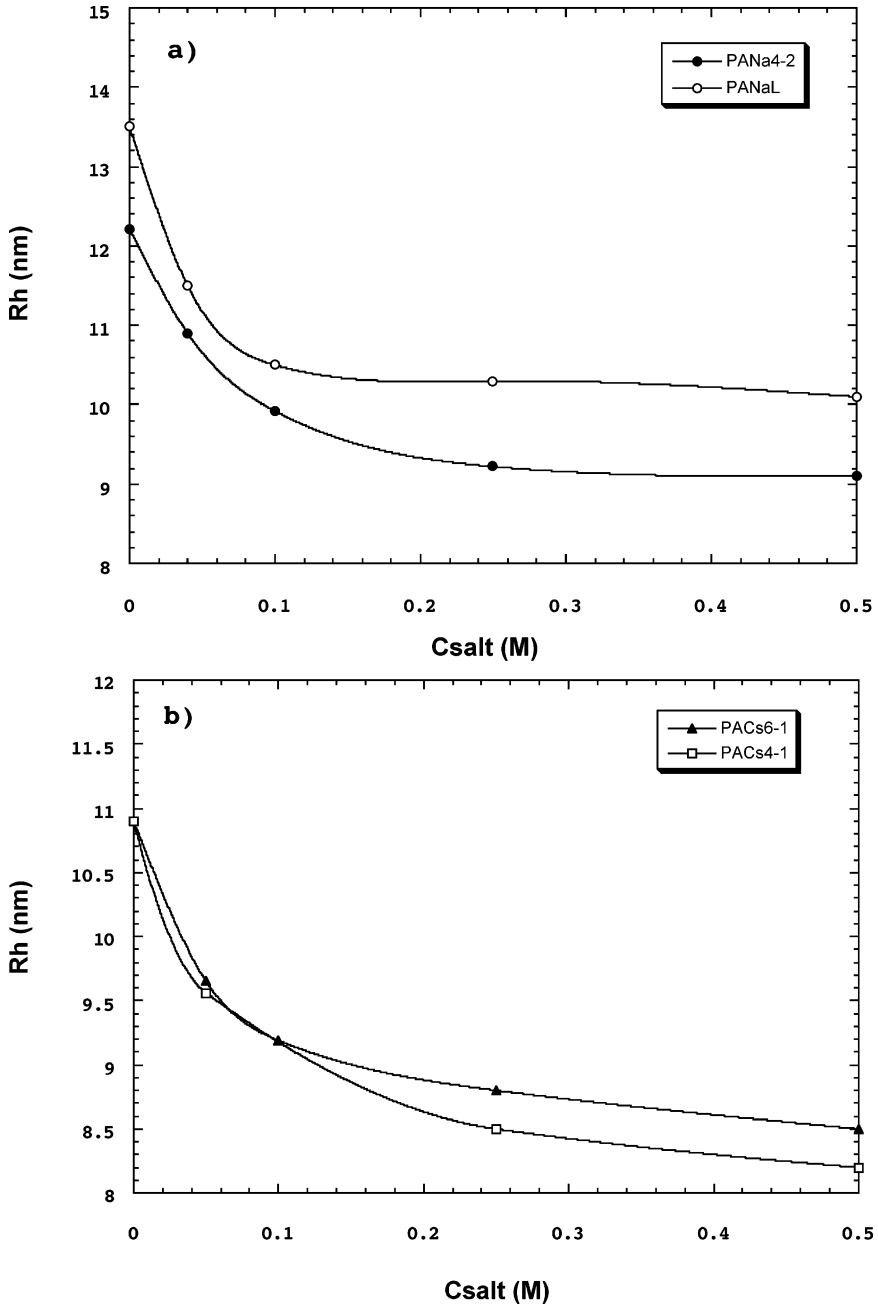

Figure 6. (a) C_{salt} effect on R_H for four-arm star and linear equivalent of polysodium acrylate. (b) C_{salt} effect on R_H for six-arm star and four-arm star equivalent of polycesium acrylate.

behavior of a rodlike molecule. The determination of the persistence length L_p is related to the value q^* at which $qP(q)$ reaches a plateau. This relation, however, holds for Θ solvent. In a good solvent as in our case, the excluded-volume effect is not an issue at the local scale of the chain and high q value, as previously shown using Monte Carlo simulations.[53] Therefore, we have used this method and a good approximation of relation 11; i.e., $q^*L_p \cong 3.5$ to estimate the persistence length.

This is illustrated in Figure 8 where $qI(q)$ is plotted as a function of q. In this case, q^* is the value for which a plateau appears and the persistence length can be estimated using the relation $q^*L_p \cong 3.5$.[50] From these plots, q^* could be extracted and the corresponding persistence length of each system be calculated using the different methods described above. The obtained values are summarized in Table 5 and compared to the ones obtained using light scattering experiments.

It turns out that the persistence length of linear systems is lower than that of the polyelectrolyte stars, whatever the scattering technique used (light or X-ray scattering). According to the values listed in Table 5, one can consider that the two approaches (SAXS, LS) give comparable results. As a matter of fact, the agreement between light and X-ray scattering data is found better for a Kratky representation with $k = 1.91$.

III.4. Reduced Viscosity in "Salt-Free" Solutions. The peculiar behavior of the viscosity of linear polyelectrolytes such as sodium polystyrenesulfonate (NaPSS) has been already studied by different authors including, Hodgson et al.,[38] Yamanaka,[54] or Cohen[39,55] and their collaborators. In this section, the viscosity of star polyelectrolyte solutions PANa, PACs, and PARb is investigated and compared with the behavior of their linear counterparts and with that of the most studied system NaPSS. The responses of very dilute linear

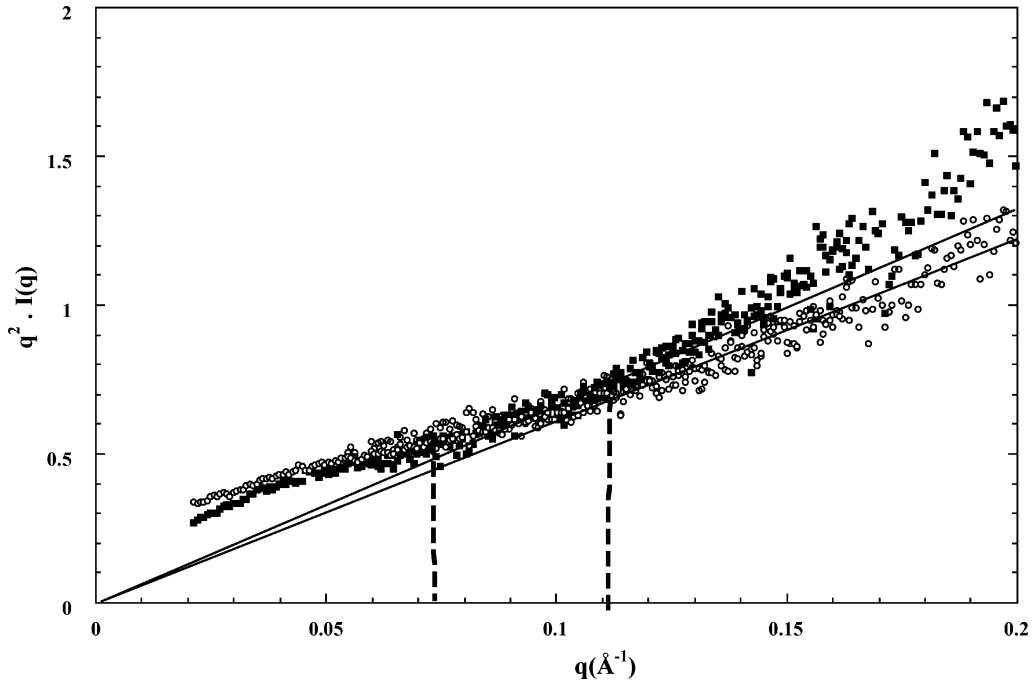

Figure 7. Kratky plot $q^2I(q)$ as a function of q: (○) PANaL C_P = 10 mg/mL, C_{salt} = 0.5 M; (●) PANa4-2 C_P = 10 mg/mL, C_{salt} = 0.5 M.

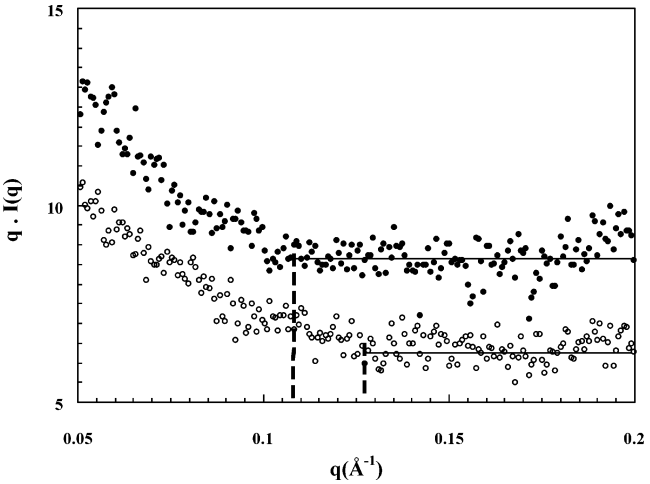

Figure 8. des Cloiseaux representation $qI(q)$ as a function of q: (○) PANaL C_P = 10 mg/mL, C_{salt} = 0.5 M; (●) PANa4-2 C_P = 10 mg/mL, C_{salt} = 0.5 M.

NaPSS solutions to steady shear rate experiments were first studied. The variation of the solution viscosity η vs the shear rate γ (Figure 9) shows no dependence of the viscosity with shear rate γ (Newtonian plateau).

From these results, η_{red}, defined as $(\eta - \eta_0)/\eta_0 C_P$, was plotted as a function of the polyelectrolyte concentration C_P and compared to earlier results from Cohen et al.[39] (see Figure 10).

As expected, η_{red} increases with decreasing C_P and shows a maximum for very dilute solutions at exactly the same concentration found by Cohen et al.[39] As shown in different investigations,[17,38,39] this peak position is independent of the molar mass of the polymer and is very sensitive to the presence of free ions in excess of salt.[14,38,41] This implies that the electrostatic interactions are at the origin of this observed maximum. As mentioned in the Introduction, this peak is usually explained by the expansion of the polyelectrolyte chains. The dilution of polyelectrolyte solution causes the decrease of the total ionic strength leading to an increase of the distance over which the electrostatic interactions are present. Hence, the chain expansion phenomenon of polyelectrolyte appears to be due to the increase of intermolecular interactions. In this study, we have measured the reduced viscosity of polyelectrolyte chains having a star architecture in order to determine whether these systems presented a similar behavior to that of their linear equivalents.

Thus, the reduced viscosity of the PANa4-2 star and that of the linear equivalent PANaL (having the same molar mass) as well as the η_{red} of PARb4-3 and PARbL have been studied (Figure 11). In all cases, the reduced viscosity η_{red} increases when the polyelectrolyte concentration decreases and is found smaller for the star case. One also observes that the maximum in the reduced viscosity is found at the same polyelectrolyte concentration for both linear and star polyelectrolyte systems carrying the same counterion. This position of the maximum of the reduced viscosity η_{red} as a function of C_P depends on the counterion nature (see the discussion below). For linear systems, the increase of η_{red} is more pronounced than in the case of the star systems. Since the increase and the maximum of the reduced viscosity are related to the polyelectrolyte chains expansion phenomenon, the different observed behaviors for the star and the linear are due either to the charge parameter or to the architecture itself.

To ensure the electroneutrality in polyelectrolyte solutions, counterions have to be present. It is energetically or thermodynamically advantageous that a fraction of counterions "condense" to the surface of the polyion to reduce the effective charge parameter. Such a concept of counterion association/condensation was introduced by Fuoss, Katchalsky, Lifson, and Oosawa and ultimately modeled by Manning,[56,57] known as the Manning condensation. The "two-state" model of Manning is frequently used and the condensation or Manning parameter is defined as $\Lambda = l_B/b$, where b is the charge distance. For $l_B/b > 1$, the electrostatic effect dominates

Table 5. Values of L_p for PANa Star and Linear Polyelectrolyte System Measured in Excess of Salt as a Function of k Using Different Methods (Light Scattering and X-ray Scattering)

scattering technique	method	k in $L_p' = k/q^*$	L_p (nm) PANaL	L_p (nm) PANa4-2
X-ray	Kratky	1.91	1.74 ($q^* = 0.11$)	2.62 ($q^* = 0.073$)
		2.87	2.61 ($q^* = 0.11$)	3.93 ($q^* = 0.073$)
	des Cloiseaux	3.5	2.77 ($q^* = 0.126$)	3.24 ($q^* = 0.108$)
light	Reed		1.87	2.7

and the counterion condensation occurs, whereas for $l_B/b < 1$, the entropy dominates and the counterions can move freely in the solution—no counterions condensation.

Therefore, because of the Manning condensation—e.g., distance between consecutive counterions: Bjerrum length (∼7 Å in water at 25 °C)—only one counterion over 3 is dissociated and the other 2/3 are condensed on the chains. Therefore, the effective charge parameter τ_{eff} is the same for all the studied star systems. Consequently, the difference of the reduced viscosity behavior is due only to the chain architecture. Since this maximum is due to an expansion phenomenon of the polyelectrolyte chains, this difference can be explained by the fact that linear and star polyelectrolyte chains do not expand similarly. In fact, one can consider the four-arm polyelectrolyte stars as two linear polyelectrolyte chains linked together in their middle monomer

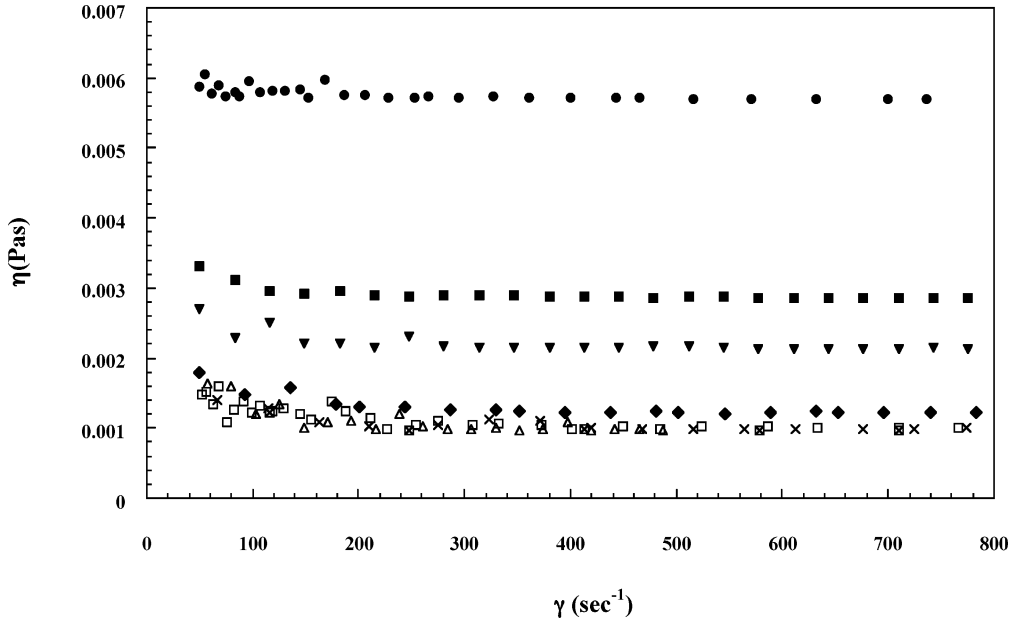

Figure 9. Viscosity η of "salt-free" aqueous NaPSS solutions vs shear rate γ for different polyelectrolyte concentration C_P: (●) 5, (■) 1, (▼) 0.5, (◆) 0.1, (□) 0.01, (×) 0.002, (⊞) 0.001, and (△) 0.0005 mg/mL.

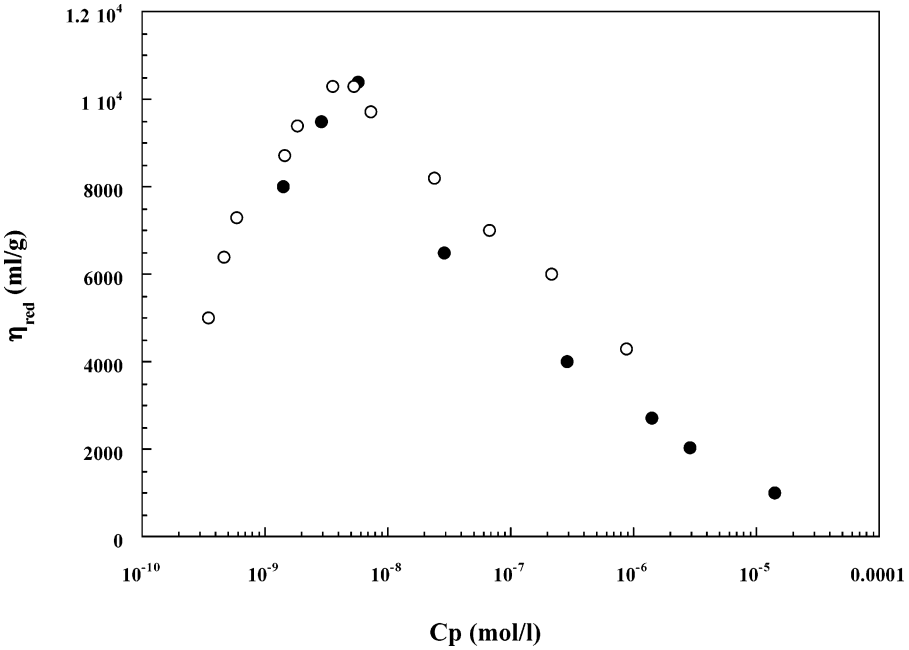

Figure 10. Reduced viscosity η_{red} of "salt-free" aqueous NaPSS solutions as a function of polyelectrolyte concentration C_P (given in mol/L): ●, our experimental data (M = 350 000 g/mol); ○, Cohen et al. data (M = 345 000 g/mol).[29]

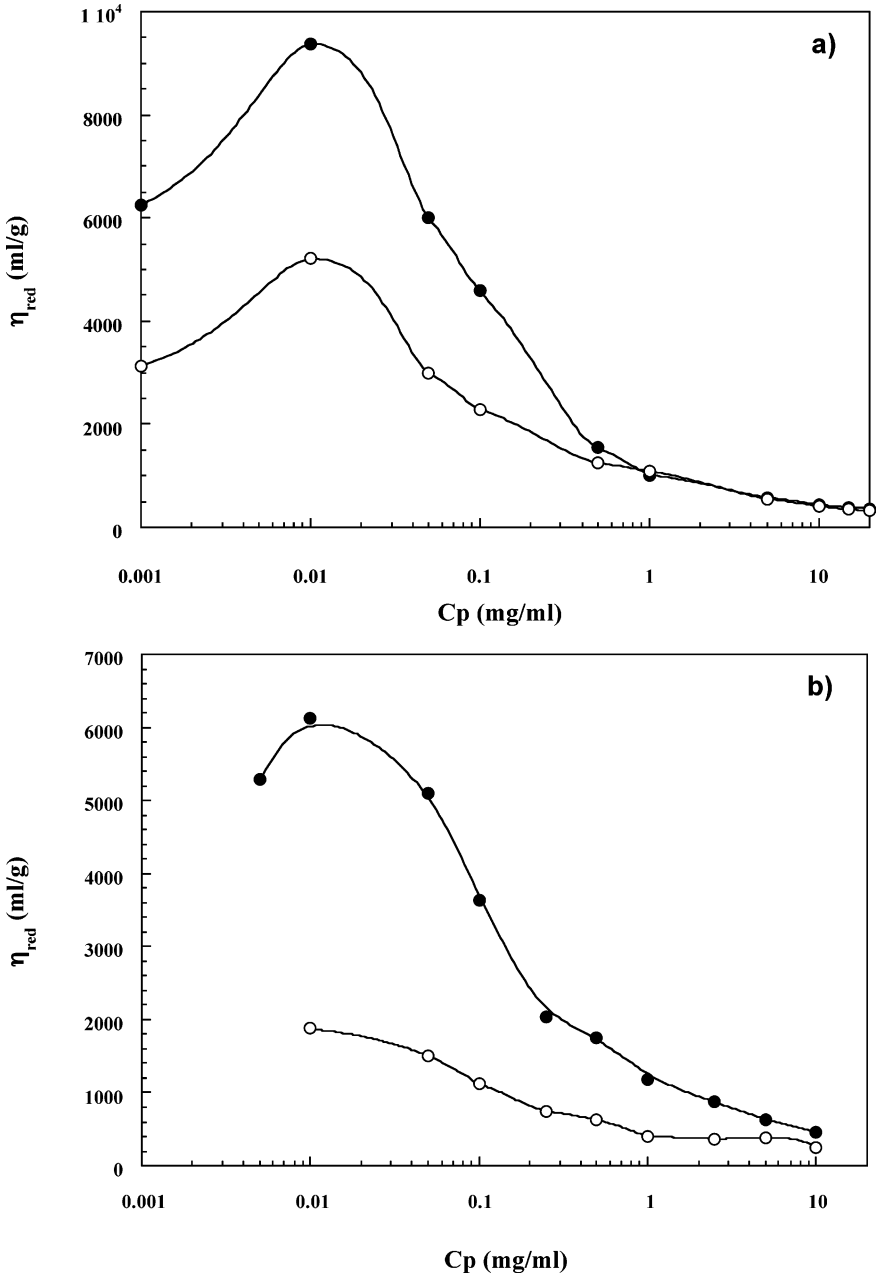

Figure 11. (a) Reduced viscosity η_{red} of "salt-free" aqueous star and linear polyelectrolyte solutions (having the same degree of polymerization) as a function of polyelectrolyte concentration C_P. ●, PANaL (DP = 840); ○, PANa4-2 (DP = 860). (b) Reduced viscosity η_{red} of "salt-free" aqueous star and linear polyelectrolyte solutions (having the same degree of polymerization) as a function of polyelectrolyte concentration C_P. ●, PARbL (DP = 992); ○, PARb4-3 (DP = 937).

unit. Therefore, because of the presence of the star core, the chain expansion is less important for polyelectrolyte star chains than linear ones that do not present such sterical constraints.

For polyelectrolyte star systems with different molar masses, PANa4-2 and PANa4-1 (Figure 12), the same behavior was observed, the maximum being more pronounced for the highest molar mass, i.e., PANa4-2. This result shows that expansion is proportional to the molar mass.

Similar results were obtained with polycesium acrylate stars having the same functionality and different molar masses: PACs4-1/PACs4-2 (Figure 13). The reduced viscosity of the six-arm star having the same molar mass as that of the four-arm star is also illustrated in Figure 12 (PANa4-1/PANa6-1) and Figure 13 (PACs4-1/PACs6-1). For all studied concentrations, the η_{red} of four-arm star is slightly higher than that of six-arm star. This result again can be explained on the basis of PANa6-1 and PACs6-1 having a lower degree of freedom of chains as compared to 4-arm stars or linear polyelectrolytes. It is important to note that for polysodium or polycesium acrylate systems the maximum appears at the same polyelectrolyte concentration. The nondependence of the reduced viscosity position as a function of C_P for different molar mass has been already observed by several authors and indicates that the viscosity maximum does not arise from intermolecular entanglements. This is confirmed by the fact that these maxima are also independent of the shape of the polyelectrolyte (linear or star). Figure 14 presents η_{red} as a function of C_P for 4-arm stars having approximately the same degree of polymerization and different counterions (Na, Cs, Rb).

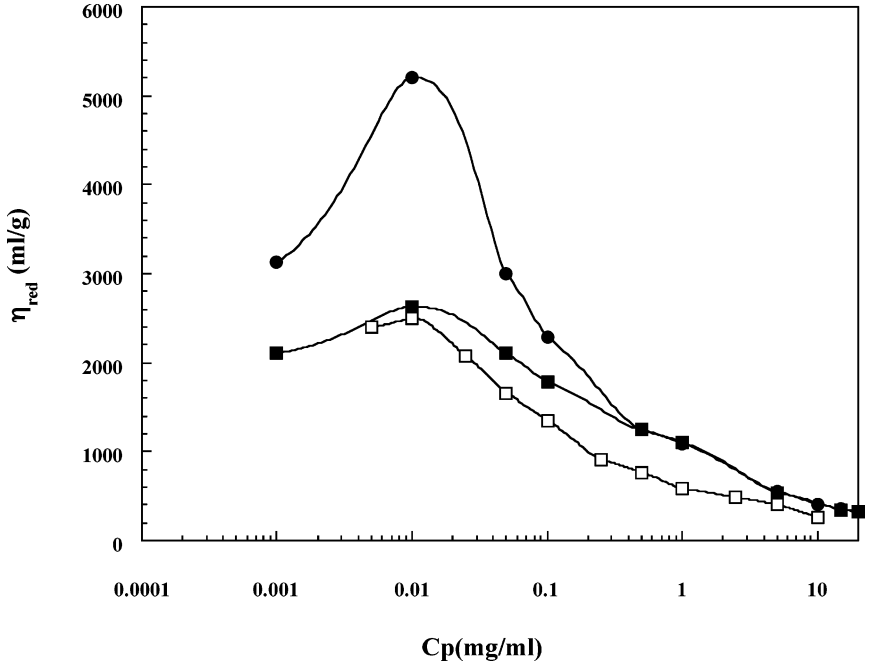

Figure 12. Reduced viscosity η_{red} of "salt-free" aqueous PANa star polyelectrolyte solutions as a function of the polyelectrolyte concentration C_P: ●, PANa4-2 (DP = 860); ■, PANa4-1 (DP = 617); □, PANa6-1 (DP = 624).

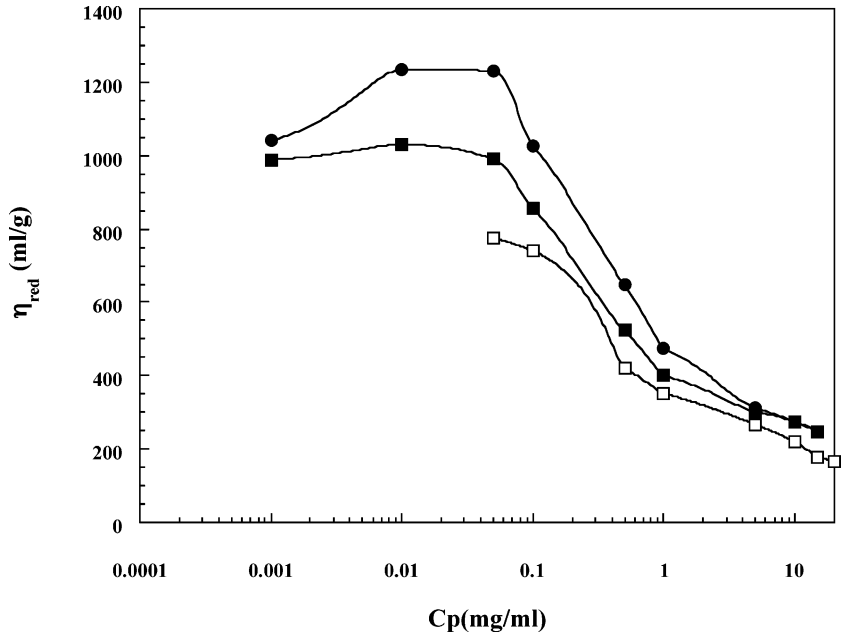

Figure 13. Reduced viscosity η_{red} of "salt-free" aqueous PACs star polyelectrolyte solutions as a function of polyelectrolyte concentration C_P: ●, PACs4-2 (DP = 860); ■, PACs4-1 (DP = 617); □, PACs6-1 (DP = 624).

It is more difficult to explain the difference between the behavior of PANa and PACs stars (having the same degree of polymerization), in particular the position of the maximum on the basis of the expansion of chains only. The main difference between these three systems is the counterion nature since the effective charge parameter is the same (Manning condensation). At the same concentration, one observes that $\eta_{red,PACs4-2} < \eta_{red,PARb4-3} < \eta_{red,PANa4-2}$: the smaller the counterion size, the larger the η_{red} maximum. Since the charge parameter is the same for the systems studied, the difference in η_{red} can be explained by the interaction between polyion chains and counterions (since the backbone and the solvent are the same). The counterion influence on polyelectrolyte systems (including ionomers systems) has been studied by measuring the activity coefficient, the conductimetric, or the viscosimetric study in dilute regime.[58−60] Nevertheless, to our knowledge, the counterion influence on η_{red} maximum has never been clearly shown since no experimental study has been carried out in very dilute polyelectrolyte concentration range. Regarding the polyelectrolyte systems with sulfonated charged groups, the interaction between counterion and polyion Ψ_{cp} increases as the counterion size decreases ($\Psi_{cp,Li} > \Psi_{cp,Na} > \Psi_{cp,K}$ ...), whereas for polyelectrolyte systems having carboxylate charged groups, the interaction are completely different since in this case Ψ_{cp} increases when the counterion size increases ($\Psi_{cp,Li} < \Psi_{cp,Na} < \Psi_{cp,K}$ ...). By studying the reduced viscosity of ionomers systems in DMF (sulfonated and carboxylated

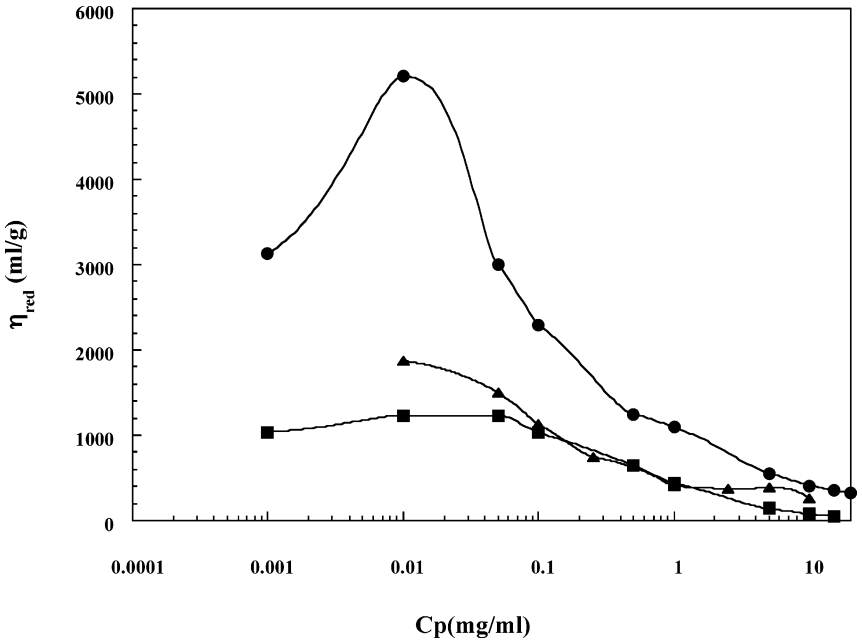

Figure 14. Reduced viscosity η_{red} of "salt-free" aqueous PANa, PACs, and PARb star polyelectrolyte solutions (having similar DP) as a function of polyelectrolyte concentration C_P: ●, PANa4-2 (DP = 860); ■, PACs4-2 (DP = 860); ▲, PARb4-3 (DP = 937).

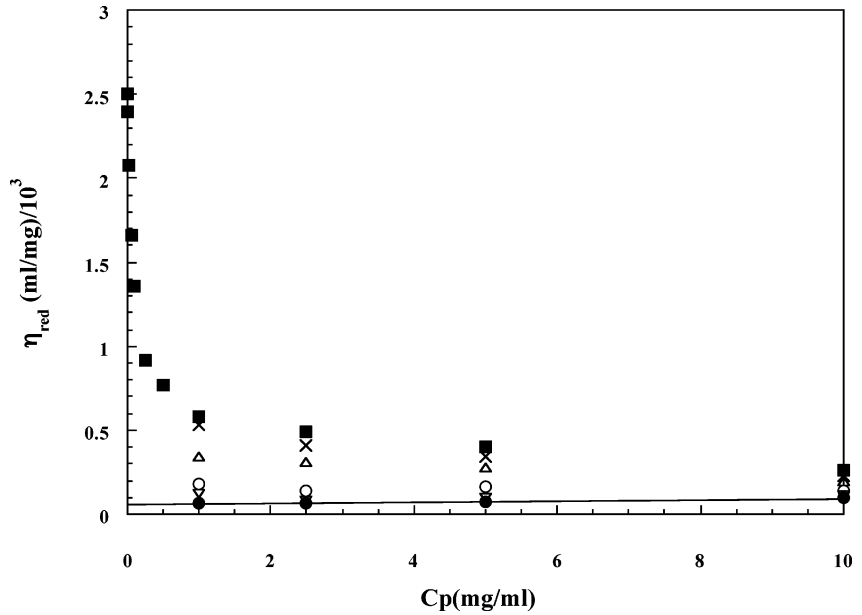

Figure 15. Typical effect of added salt on η_{red} of PANa6-1 polyelectrolyte solutions. Curves of η_{red} as a function of polyelectrolyte concentration C_P for polyelectrolyte star solutions at different added salt concentration C_{salt}: (■) 0, (×) 0.005, (△) 0.01, (○) 0.05, (▽) 0.1, and (●) 0.5 M.

ionomers), Hara et al.[61] did not observe the same order regarding the interaction between counterion and polyion. It is important to note that Hara's results have been obtained in polar organic solvent (DMF) and not in aqueous solvent. DMF and water are two polar solvents; the first is aprotic whereas the second is protic. This difference might not explain the observed difference regarding counterion/polyion interaction, and these different results (ionomers/polyelectrolytes) are difficult to account for. In our case, the decrease of η_{red} when the counterion size increases can be explained as follows: the stronger the counterion/polyion interaction, the smaller the electrostatic repulsive interactions due to the counterion, the latter forming a "shield" between the charges of polyion. Electrostatic repulsive interactions between the chain charges decrease and lead to a global diminution of chain size that in turn induces a decrease of the reduced viscosity. Hence, in our case, the Ψ_{cp} interactions seem to be stronger for the larger counterion.

III.5. Reduced Viscosity of Polyelectrolyte Star Solutions in the Presence of Added Salt. With the addition of added salt such as NaCl, electrostatic effects are suppressed. Because of the fact that the charged groups of the polymer chains are neutralized, polymers adopt the behavior of neutral chains, allowing one to determine $[\eta]$ by the extrapolation of η_{red} to $C_P = 0$. Typical behaviors of η_{red} as a function of C_P at different ionic strengths are illustrated in Figure 15 for PANa6-1 stars. With the addition of a simple electrolyte, the maximum of η_{red} disappears. η_{red} varies with the ionic strength and becomes approximately constant when

Table 6. Determination of $[\eta]$, R_V (nm), and R_V/R_g

	linear		four-arm star			six-arm star	
	PANaL	PARbL	PANa4-1	PANa4-2	PARb4-3	PANa6-1	PACs6-1
$[\eta]$ (mL/mg)	0.162	0.163	0.118	0.124	0.119	0.065	0.053
k_H	0.5	0.4	0.53	0.43	0.45	0.77	0.68
R_V (nm)	13.27	13.99	9.78	11.12	11.48	8.42	8.57
R_g (nm)	18.1	19	14	16.1	15.6	13.7	14.2
R_V/R_g	0.73	0.73	0.69	0.69	0.73	0.61	0.60
	1.36	1.35	1.43	1.44	1.35	1.62	1.65

Table 7. Experimental and Theoretical g' Values

system	$[\eta]$ (mL/mg)	$g'_{exp} = [\eta]_{étoile}/[\eta]_{linear}$	g'_{Zimm}	g'_{Fixman}	$g'_{Roovers}$
PANaL	0.162		0.82	0.71	0.76
PANa4-1	0.118	0.73			
PANa4-2	0.124	0.76			
PARbL	0.163				
PARb4-3	0.119	0.72			
PANaL	0.162		0.7	0.51	0.55
PANa6-1	0.065	0.4			

enough salt is added (i.e., when all charges are screened). By extrapolation of η_{red} to $C_P = 0$, the intrinsic viscosity $[\eta]$ could be determined for all the studied systems: $[\eta]_{PANaL} = 0.162$, $[\eta]_{PANa4-1} = 0.118$, $[\eta]_{PANa4-2} = 0.124$, $[\eta]_{PANa6-1} = 0.065$, $[\eta]_{PARbL} = 0.163$, and $[\eta]_{PARb4-3} = 0.119$ mL/mg. Star polymers exhibit a smaller hydrodynamic radius as compared to linear polymers of the same molar mass, and since $[\eta]$ is related to hydrodynamic radius R_H, the intrinsic viscosity is higher in the case of linear system and as expected $[\eta]_{lin} > [\eta]_{star}$; $[\eta]$ increases when the functionality decreases: $[\eta]_{PANa4-1} > [\eta]_{PANa6-1}$. Moreover, $[\eta]_{PANa4-2} > [\eta]_{PANa4-1}$ due to the fact that R_H and M are larger in the case of PANa4-2.

From the intrinsic viscosities measured in excess of salt, the viscometric radius could be calculated using the relation $R_V = [3/10\pi N_A]^{1/3}([\eta]M_{app})^{1/3}$. The results are reported in Table 6. The functionality f could also be calculated as follows: in θ solvent, different relations of g' defined as $[\eta]_{\text{branched polymer}}/[\eta]_{\text{linear polymer}}$ have been established as a function of f. The Fixman–Stockmayer[62] model proposes that

$$g' = f^{3/2}[2 - f + 2^{1/2}(f - 1)]^{-3} \qquad (13)$$

whereas Zimm and Kilb[63] model predict that

$$g' = \left(\frac{2}{f}\right)^{3/2}[0.39(f - 1) + 0.196]/0.586 \qquad (14)$$

Finally, the Roovers empirical relation[64] relates g' to f as

$$\log g' = 0.36 - 0.80 \log f \qquad (15)$$

Even if these relations have been established for θ conditions, both experimental and theoretical values of g' are very close as also shown elsewhere.[65,66] In good solvent, the expansion of branched polymer can be different compared to linear polymer, and this point can explain the little disparity between g' values in good and θ solvents. In Table 7 are listed the experimental and theoretical values of g' for investigated systems. g' was calculated for PANaL/PANa4-2 and PARbL/PARb4-3, the linear systems exhibiting the same DP as that of four-arm star systems. We also calculated g' for PANaL/PANa4-1 (DP = 840 and 617) and for PANaL/PANa6-1 (DP = 840 and 624). Despite the difference in the degree of polymerization between star and linear systems, the comparison that we made shows that g' values are very close to the predicted ones, allowing us to conclude that the synthesized stars carry effectively four and six arms, respectively.

IV. Conclusion

This paper discusses the solution properties of well-defined star-shaped polyelectrolyte systems. Four- and six-arm sodium, cesium, and rubidium polyacrylate (PANa, PACs, PARb) star polyelectrolyte, synthesized by atom transfer radical polymerization (ATRP) and chemical modifications, were investigated. A systematic comparison, using light scattering, X-ray, and viscosity experiments, between the solution properties of star-shaped and their equivalent linear polyelectrolyte is presented. Among other properties, the polyelectrolyte effect is highlighted in these systems and investigated as a function of polyelectrolyte star concentration, added salt (screening of electrostatic interactions), nature of the counterion, functionality, and molar mass.

Static light scattering experiments carried out in excess of salt allowed us to have access to molar masses and second virial coefficients and to determine the radii of gyration. A more detailed analysis of the data collected using light and X-ray scattering allows us to measure the apparent persistence length for linear polyelectrolyte systems as well as the star ones. The results found using both techniques, light[31,43] and X-rays (using the Kratky and des Cloiseaux representations), gave a reasonable agreement.

The DLS data revealed two relaxation modes: fast and slow. The fast mode identified as the single chain dynamics allows the determination of the hydrodynamic radii R_H in "salt-free" or in excess of added salt solutions. R_H was found to depend on the architecture as well as on the counterion nature.

Regarding viscosity data, the typical behavior of η_{red}, exhibiting a maximum at very low polyelectrolyte concentrations C_P, has been highlighted for both star and linear polyelectrolyte systems in "salt-free" solutions. The influence of architecture on polyelectrolytes having same molar masses, the effect of molar mass, and the influence of counterions were in particular investigated. Thus, it was proposed that the η_{red} maximum can be explained by the expansion chain phenomenon and is also related to the interaction between the counterion and the polyion. Hence, the viscosity of polyelectrolyte system depends not only on its architecture (linear, star, ...) but also on the counterion nature. In excess of salt, the results show, as expected, the disappearance of η_{red} maximum, allowing thus to determine the intrinsic viscosity and to confirm the four- and six-arm functionality of the different starlike structures.

References and Notes

(1) Liao, Q.; Dobrynin, A. V.; Rubinstein, M. *Macromolecules* **2003**, *36*, 3386−3398.
(2) Liao, Q.; Dobrynin, A. V.; Rubinstein, M. *Macromolecules* **2003**, *36*, 3399−3410.
(3) Dobrynin, A. V.; Rubinstein, M. *Macromolecules* **2001**, *34*, 1964−1972.
(4) Dobrynin, A. V.; Colby, R. H. Rubinstein, M. *Macromolecules* **1995**, *28*, 1859−1871.
(5) Foerster, S.; Schmidt, M.; Antonietti, M. *J. Phys. Chem.* **1992**, *96*, 4008−4014.
(6) Beer, M.; Schmidt, M.; Muthukumar, M. *Macromolecules* **1997**, *30*, 8375−8385.
(7) Drifford, M.; Belloni, L.; Dalbiez, J. P.; Chattopadhya, A. K. *J. Colloid Interface Sci.* **1985**, *105*, 587.
(8) Ise, N.; Okubo, T.; Kunugi, S.; Matsuoka, H.; Yamamoto, K.; Ishii, Y. *J. Chem. Phys.* **1984**, *81*, 3294−3306.
(9) Ermi, B. D.; Amis, E. J. *Macromolecules* **1998**, *31*, 7378−7384.
(10) Tanahatoe, J. J.; Kuil, M. E. *Macromolecules* **1997**, *30*, 6102−6106.
(11) Borsali, R. In *Handbook of Polyelectrolytes and Their Applications*; Tripathy, S. K., Kumar, J., Nalwa, S., Eds.; American Scientific Publishers: Los Angeles, 2002; pp 249−265.
(12) Hess, W.; Klein, R. *Adv. Phys.* **1983**, *32*, 173.
(13) Rabin, Y.; Cohen, J.; Priel, Z. *J. Polym. Sci.*, *Part C* **1988**, *26*, 397−399.
(14) Borsali, R.; Vilgis, T. A.; Benmouna, M. *Macromolecules* **1992**, *25*, 5313−5317.
(15) Hodgson, D. F.; Amis, E. J. *J. Chem. Phys.* **1991**, *94*, 4581−4586.
(16) Boris, C. D.; Colby, R. H. *Macromolecules* **1998**, *31*, 5746−5755.
(17) Antonietti, M.; Briel, A.; Förster, S. *J. Chem. Phys.* **1996**, *105*, 7795−7807.
(18) Odijk, T. *Macromolecules* **1979**, *12*, 688−693.
(19) Borisov, O. V. *J. Phys. II* **1996**, *6*, 1−19.
(20) Wolterink, J. K.; Leermakers, F. A. M.; Fleer, G. J.; Koopal, L. K.; Zhulina, E. B.; Borisov, O. V. *Macromolecules* **1999**, *32*, 2365−2377.
(21) Borisov, O. V.; Daoud, M. *Macromolecules* **2001**, *34*, 8286−8293.
(22) Heinrich, M.; Rawiso, J. M.; Zilliox, G.; Lesieur, P.; Simon, J. P. *Eur. Phys. J. E* **2001**, *4*, 131−142.
(23) Moinard, D.; Taton, D.; Gnanou, Y.; Rochas, C.; Borsali, R. *Macromol. Chem. Phys.* **2003**, *204*, 89−97.
(24) Furukawa, T.; Ishizu, K. *Macromolecules* **2005**, *38*, 2911−2917.
(25) Furukawa, T.; Ishizu, K. *Macromolecules* **2003**, *36*, 434−439.
(26) Mishra, K.; Kobayashi, S. *Star and Hyperbranched Polymers*; M. Dekker: New York, 1999.
(27) Hadjichristidis, N.; Pitsikalis, M.; Pispas, S.; Iatrou, H. *Chem. Rev.* **2001**, *101*, 3747.
(28) Matyjaszewski, K.; Miller, P. J.; Pyun, J.; Kickelbick, G.; Diamanti, S. *Macromolecules* **1999**, *32*, 6526.
(29) Ueda, J.; Matsuyama, M.; Kamigaito, M.; Sawamoto, M. *Macromolecules* **1998**, *31*, 557.
(30) Angot, S.; Murthy, S. K.; Taton, D.; Gnanou, Y. *Macromolecules* **1998**, *31*, 7218−7225.
(31) Reed, W. F.; Ghosh, S.; Medjahdi, G.; Francois, J. *Macromolecules* **1991**, *24*, 6189−6198.
(32) Skolnick, J.; Fixman, M. *Macromolecules* **1977**, *10*, 944−948.
(33) Tricot, M. *Macromolecules* **1984**, *17*, 1698−1704.
(34) Muroga, Y.; Noda, I.; Nagasawa, M. *Macromolecules* **1985**, *18*, 1576−1579.
(35) Schmidt, M. *Macromolecules* **1991**, *24*, 5361−5364.
(36) Fuoss, R. M. *J. Polym. Sci., Part B* **1948**, *3*, 603.
(37) Eisenberg, H.; Pouyet, J. *J. Polym. Sci.* **1954**, *13*, 85.
(38) Hodgson, D. F.; Amis, E. J. In *Polyelectrolytes Science and Technology*, Hara, M. Ed.; Marcel Dekker: New York, 1993; pp 127−191.
(39) Cohen, J.; Priel, Z.; Rabin, Y. *J. Chem. Phys.* **1988**, *88*, 7111.
(40) Yamanaka, J.; Matsuoka, H.; Kitano, H.; Hasegawa, M.; Ise, N. *J. Am. Chem. Soc.* **1990**, *112*, 587−592.
(41) Borsali, R. *Macromol. Chem. Phys.* **1996**, *197*, 3947−3994.
(42) Zimm, B. H. *J. Chem. Phys.* **1948**, *16*, 1099.
(43) Villetti, M. A.; Borsali, R.; Crespo, J. S.; Soldi, V.; Fukada, K. *Macromol. Chem. Phys.* **2004**, *205*, 907.
(44) Kitano, T.; Taguchi, A.; Noda, I.; Nagasawa, M. *Macromolecules* **1980**, *13*, 57−63.
(45) Lin, S. C.; Lee, W. I.; Schurr, J. M. *Biopolymers* **1978**, *17*, 1041.
(46) Sedlak, M.; Amis, E. J. *J. Chem. Phys.* **1992**, *96*, 817−825.
(47) Sedlak, M. *Langmuir* **1999**, *15*, 4045−4051.
(48) Kratky, O. *Kolloid-Z.* **1962**, *182*, 7.
(49) Cloiseaux, D. *Macromolecules* **1973**, *6*, 403.
(50) Lecommandoux, S.; Chécot, F.; Borsali, R.; Schappacher, M.; Deffieux, A.; Brulet, A.; Cotton, J.-P. *Macromolecules* **2002**, *35*, 8878−8881.
(51) Koyama, R. *J. Phys. Soc. Jpn.* **1973**, *34*, 1029.
(52) Burchard, W.; Kajiwara, R. *Proc. R. Soc. London*, *A* **1970**, *316*, 185.
(53) Zimm, H.; Le Bret, M. *Biopolymers* **1984**, *23*, 271.
(54) Yamanaka, J.; Araie, H.; Matsuoka, H.; Kitano, H.; Ise, N.; Yamaguchi, T.; Saeki, S.; Tsubokawa, M. *Macromolecules* **1991**, *24*, 6156−6159.
(55) Cohen, J.; Priel, Z.; Rabin, Y. *J. Chem. Phys.* **1988**, *29*, 235.
(56) Manning, G. S. *J. Chem. Phys.* **1969**, *51*, 924.
(57) Manning, G. S. Q. *Rev. Biophys.* **1978**, *11*, 179−246.
(58) Ross, P. D.; Strauss, U. P. *J. Am. Chem. Soc.* **1960**, *82*, 1311−1314.
(59) Hen, J.; Strauss, U. P. *J. Phys. Chem.* **1974**, *78*, 1013−1017.
(60) Armstrong, R. W.; Strauss, U. P. *Encycl. Polym. Sci. Technol.* **1969**, *10*, 781.
(61) Hara, M.; Lee, A. H.; Wu, J. *J. Polym. Sci.*, *Part B* **1987**, *25*, 1407−1418.
(62) Stockmayer, W. H.; Fixman, M. *Ann. N.Y. Acad. Sci.* **1953**, *57*.
(63) Zimm, H.; Kilb, W. *J. Polym. Sci.* **1959**, *37*, 19.
(64) Roovers, J. In *Star and Hyperbranched Polymers*; Mishra, M. K., Kobayashi, S., Eds.; Marcel Dekker: New York, 1999; pp 285−341.
(65) Burchard, W. *Adv. Polym. Sci.* **1999**, *143*, 113−194.
(66) Bywater, S. *Adv. Polym. Sci.* **1979**, *30*, 89−116.

MA050505F